A low noise transimpedance amplifier for cryogenically cooled quartz tuning fork force sensors

C. H. Yang[a] and T. H. Chang
Department of Electrical and Computer Engineering, University of Maryland, College Park, Maryland 20742

M. J. Yang
Naval Research Laboratory, Washington, DC 20375

W. J. Moore
SFA, Inc., Largo, Maryland 20774

(Received 3 January 2002; accepted for publication 23 April 2002)

We have designed and built a low noise, broadband transimpedance amplifier that allows for sensing both the amplitude and phase of an oscillating quartz tuning fork for a cryogenic atomic force microscope. The circuit uses a global feedback scheme, where the input stage, located next to the quartz tuning fork at low temperature, is followed by an operational amplifier stage operated at room temperature. At 4.2 K, with a 1 MΩ metal film feedback resistor, the amplifier yields an output noise floor of 2×10^{-7} V/$\sqrt{\text{Hz}}$ and a bandwidth of 200 kHz. When it is used with a commercial 32 kHz quartz tuning fork, the calibrated sensitivity at 4.2 K is determined to be 30.8 μV/pm. © *2002 American Institute of Physics.* [DOI: 10.1063/1.1487890]

I. INTRODUCTION

The atomic force microscope (AFM) uses a force-sensing cantilever, whose deformation is monitored by a laser as a feedback signal for topographic imaging.[1] A frequency modulation technique using a high Q cantilever has been shown to have advantages such as a large signal to noise ratio and a high bandwidth.[2] The piezoelectric quartz tuning forks (QTFs) are low cost, stiff, high in Q, and they provide self-sensing. Therefore, the use of quartz tuning fork in near-field scanning-optical microscope[3] or AFM[4] systems has attracted a lot of interest. In these scanning probes, an oscillating QTF interacts with the sample surface. Changes in the resonance frequency, the oscillation amplitude, or phase can be used for feedback control. The QTF can be mechanically shaken[5] by a piezoelectric dither, and the induced voltage across the two tines is measured. Alternatively, the QTF can be driven by a voltage with a frequency close to its resonance frequency, and the induced current is monitored.[4] We prefer the latter, because in our AFM system the tuning fork is mounted at the end of the scanner tube. We found that the vibration of a dither mechanically couples to the scanner tube and often interferes with the raster scan function.

Operating an AFM at low temperatures allows observation of phenomena with a reduced thermal excitation energy.[6] However, the use of cryostats has an associated high (resistance–capacitance) time constant caused by long or thin signal wires. As will be discussed later, the large capacitance from the signal wires induces excess noise and reduces the bandwidth. Based on published data, a resonantly driven quartz tuning fork typically generates a voltage signal of ~10 μV,[7] or a current signal of ~1 nA.[8] Our specific goal is to develop a transimpedance amplifier for measuring both the amplitude and phase of the alternating current in response to the excitation voltage. The amplifier must be located in close proximity to the quartz tuning fork. In the following, we will present the circuit design, construction, and its characteristics.

II. THE TRANSIMPEDANCE AMPLIFIER CIRCUIT

The circuit schematic is shown in Fig. 1. The portion enclosed in the dashed box is to be cooled to 4.2 K. There are two stages. The first is a source follower, which provides a low output impedance, high input impedance, and a wide bandwidth. The characteristic low output impedance is useful in driving a 50 Ω coaxial cable. The second stage is a low noise, wide band operational amplifier with a large voltage gain. The feedback loop is completed by resistance R_f (see Fig. 1). Similar two-stage transimpedance amplifiers have been used for high impedance infrared detector amplifier at lower frequencies.[9] The principle of global feedback is explained in the following. Let $A_1(\omega)$ and $A_2(\omega)$ be the voltage gains of two amplifiers in series. With an R_f feeding the output of A_2 to the input of A_1, the transfer function with the shunt–shunt feedback configuration can be derived to be

$$\frac{V_{\text{output}}(\omega)}{I_{\text{input}}(\omega)} = -R_f\left[\frac{A_1(\omega)A_2(\omega)}{1+A_1(\omega)A_2(\omega)}\right]. \tag{1}$$

The gain is $-R_f$ when $A_1(\omega)A_2(\omega)\gg1$, and this is usually the case until the frequency is near the cut off frequency of $A_1(\omega)A_2(\omega)$.

The source follower uses a single GaAs metal–semiconductor field effect transistor (MESFET). Figures 2(a) and 2(b) show the typical current–voltage characteristics of the MESFET at room temperature and at 4.2 K, respectively. In comparison with its room temperature characteristics, the

[a]Author to whom correspondence should be addressed; electronic mail: yang@eng.umd.edu

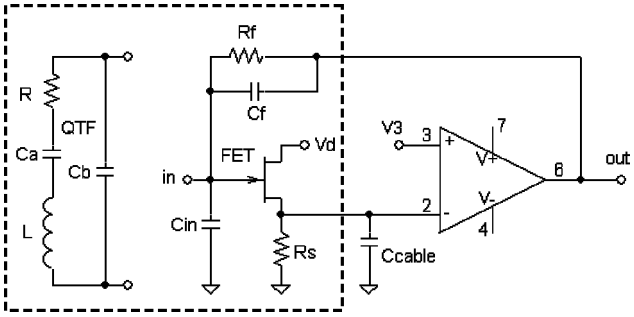

FIG. 1. The circuit diagram of the discussed amplifier. Enclosed in the dashed box is the quartz tuning fork and the first source-follower stage. For observing the thermal mechanical noise, the "in" terminal is shorted to the QTF.

current–voltage relation at 4.2 K becomes more nonlinear, and the transconductance decreases. Nonetheless, the direct current (dc) bias point of the source follower can be accurately determined once R_s and V_d are given. Because of its less-than-unity voltage gain, the bandwidth of a source follower is extended to the cutoff frequency of the transistor. For example, with $R_s = 100\ \Omega$ and $V_d = 2$ V, the voltage gain is 0.4, but the bandwidth extends beyond 100 MHz. We use an OPA602 operational amplifier as the second stage, for it offers a reasonably high gain-bandwidth product and low noise. As shown in Eq. (1), what counts is a large $A_1(\omega)A_2(\omega)$. The nonlinearity and less-than-unity voltage gain of the first MESFET stage are unimportant here, because of the use of feedback and the high gain of OPA602.

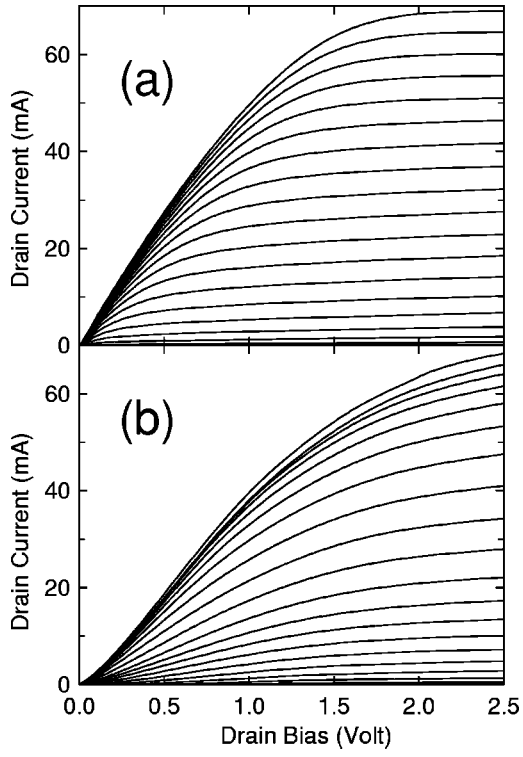

FIG. 2. The MESFET characteristics in the common source configuration at (a) 300 and (b) 4.2 K. The drain current is shown as a function of a sweeping drain bias and the gate bias is ranged from 0 (fully on, high drain current) to −2 V (zero drain current), with −0.1 V per step. The transistor, 3SK188, is a depletion mode, *n*-channel GaAs MESFET.

In operation, the dc offset at the noninverting input of the operational amplifier, V3, is first adjusted to nullify the output voltage for convenience. Both the feedback resistor and the gate bias resistor have a built-in parallel capacitive component of approximately 0.2 pF. The transimpedance gain of the entire amplifier is characterized by sending a known i_{input} to the input, and the output voltage is measured to be approximately $-i_{\text{input}}R_f$ at low frequencies. The bandwidth is determined by the impedance of the feedback resistor, the frequency response of the amplifiers, and the impedance at the input. The bandwidths, measured by HP4194A gain-phase analyzer, are found to be 10, 44, and 200 kHz, respectively, for $R_f = 100$ MΩ (carbon film), 10 MΩ (metal film), and 1 MΩ (metal film). These resistors typically have a parallel capacitance of at least 0.2 pF from packaging. (But the actual equivalent circuit is more complicated.)

The resonance frequency of the QTF[10] is measured by an impedance analyzer (HP4194A) to be ~32 768 Hz at 300 K, and ~32 711.5 Hz at 4.2 K. Based on the standard equivalent circuit shown in Fig. 1, a fitting to the measured impedance provides these components: $R = 2.098\,03$ kΩ, $C_a = 4.017\,11$ fF, $L = 5.892\,77$ kH, and $C_b = 1.763\,09$ pF. Q at 4.2 K is calculated to be $\sim 5.77 \times 10^5$.

III. NOISE CHARACTERISTICS

With a QTF as the only load at the input, we have measured the noise spectral density (NSD) (in V^2_{rms}/Hz) at the voltage output for a variety of operating conditions by a dynamic signal analyzer (HP35665A). The QTF does not bring additional signal to the noise spectra when it is off resonance, apparently due to its otherwise large internal impedance. For example, Fig. 3(a) shows the NSD for $R_f = 100$ MΩ at 300, 77, and 4.2 K. Similar noise data for $R_f = 1$ MΩ are shown in Fig. 3(b). At low frequencies, the noise reflects a $\sim 1/f^x$ feature ($x \cong 1$), inherited from the operational amplifier and the MESFET. In the flatband region, there is amplified input voltage noise, and the gain [defined to be $1/\beta(\omega)$, see Eq. (4) later] is determined by the feedback network.[11] At frequencies higher than the flatband, the noise decreases owing to the diminishing gain.[12] To understand the NSD, we have followed the standard analysis technique[9,12] and arrived at the following:

$$V^2_{\text{total,rms}}(\omega) = \left| \frac{A(\omega)}{1 + A(\omega)\beta(\omega)} \right|^2 V^2_{\text{in,rms}}(\omega) + 4k_B T R_f, \tag{2}$$

where

$$A(\omega) = \frac{A_0}{1 + \dfrac{j\omega}{\omega_0}}$$

and

$$\beta(\omega) = \frac{Z_g(\omega)}{Z_g(\omega) + Z_f(\omega)}. \tag{4}$$

Here, $V^2_{\text{total,rms}}(\omega)$ is the NSD measured at the output, $V^2_{\text{in,rms}}(\omega)$ is the equivalent input NSD at the gate terminal of the MESFET, $4k_BTR_f$ is Johnson noise of R_f, A_0 is the open

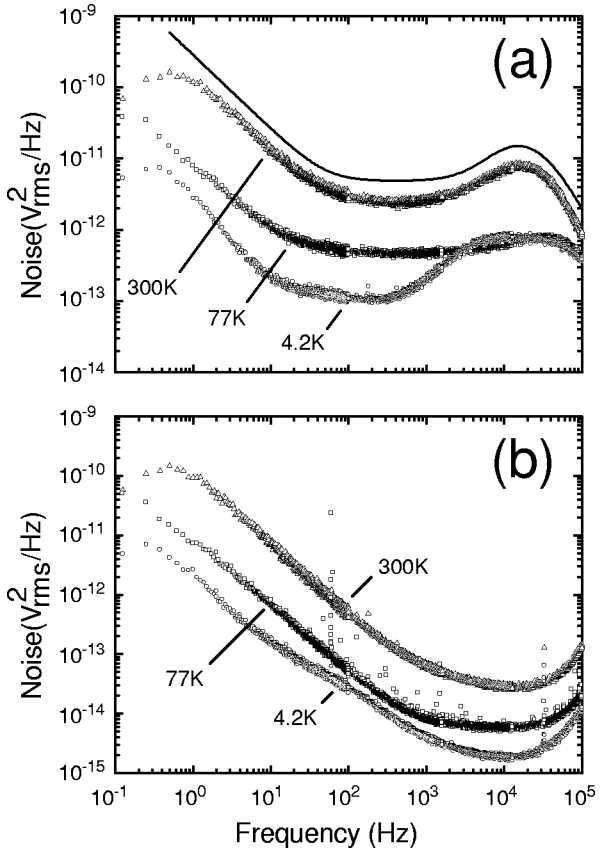

FIG. 3. The noise spectral density in $V^2_{\rm rms}$ Hz as a function of frequency from dc to 102.4 kHz for (a) $R_f = 100\ \mathrm{M}\Omega$; and (b) $R_f = 1\ \mathrm{M}\Omega$, at 300, 77, and 4.2 K. Except for the quartz oscillation near 32.768 kHz, a few spikes are identified as coming from computer, monitor, and digital switching. The solid curve in Fig. 3(a) is the simulated noise spectrum for 300 K with $R_f = 100\ \mathrm{M}\Omega$, and it is vertically offset for clarity.

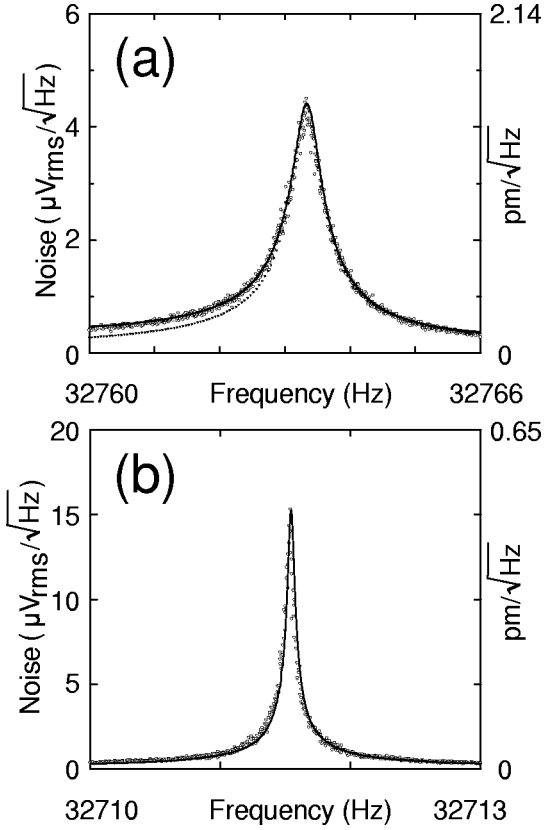

FIG. 4. The noise spectrum of a quartz tuning fork at (a) 300 and (b) 4.2 K. The circles are the measured data. The solid line is calculated by using the equivalent circuit of the QTF at the input. The dashed line is from fitting a Lorentzian line shape (predicted by the driven-damped harmonic oscillator model). The thermal vibration amplitude in pm/$\sqrt{\mathrm{Hz}}$ is obtained from normalizing the μV/$\sqrt{\mathrm{Hz}}$ scale by the sensitivity.

loop gain of the operational amplifier, ω_0 is the pole frequency of the operational amplifier, $1/\beta(\omega)$ is the noise voltage gain, $Z_g(\omega)$ is the impedance in front of the gate terminal, and $Z_f(\omega)$ is the impedance of the feedback resistor. We have numerically calculated the NSD using Eqs. (2)–(4). Take $R_f = 100\ \mathrm{M}\Omega$ at 300 K for an example, the calculated result shows excellent agreement with the measured spectrum from dc to 102.4 kHz. In the calculation, $V^2_{\rm in,rms}(\omega)$ is the sum of the spectral density of two components: (1) the equivalent input voltage noise of the operational amplifier that propagates to the gate, and (2) the drain current noise of the MESFET. According to Eq. (4), the noise gain, $1/\beta(\omega)$, defines a pole at $f_{\rm pole} = 1/(2\pi R_f C_f)$ Hz and a zero at $f_{\rm zero} = 1/[2\pi(R_f \| R_{\rm in})(C_f \| C_{\rm in})] \sim 1/[2\pi(R_f)(C_f \| C_{\rm in})]$ Hz. The impedance of the source can thus drastically influence the noise spectrum. For example, when $f_{\rm zero} < f_{\rm pole}$, the noise spectrum develops a peak near the cutoff frequency. Such peaking in noise gain near cutoff is likely to cause instability. The remedy is to minimize the noise gain in the frequency range of interest, e.g., by removing the input capacitance. As of the feedback resistor, a large R_f is preferred. Although its Johnson noise is increased, the transimpedance gain is linearly proportional to R_f, and thus the signal to noise ratio scales up as $\sqrt{R_f}$.[12] Due to the inherent parallel capacitance, the bandwidth is still limited by the time constant $R_f C_f$.

We note that a large input capacitance at the gate (labeled as $C_{\rm in}$ in Fig. 1) will likely increase the noise because that reduces Z_g and results in a higher noise gain, see Eq. (4). In our case, the printed circuit board that carries the MESFET, R_s, and R_f, can be placed less than one centimeter away from the QTF, and the $C_{\rm in}$ is limited at ~2 pF. The low output impedance (R_S in parallel with $1/g_m$) of the source follower drives the signal to OPA602 at room temperature through a 1.5 m long, 50 Ω coaxial cable. The net $C_{\rm cable}$ for miniature coaxial cables is typically more than 100 pF/m. However, using the feedback scheme reported here, $C_{\rm cable}$ is now isolated from the feedback loop, as evident from data shown later.

IV. APPLICATION ON QUARTZ TUNING FORK FOR FORCE SENSING

Adding the QTF at input allows us to directly measure its mechanical thermal noise at its resonant frequency. At 300 K, such resonance is observed near 32 768 Hz. At 4.2 K, the resonance becomes narrower and is shifted to ~32 711.5 Hz. Using $R_f = 1\ \mathrm{M}\Omega$, the noise near the resonance frequency is shown in Figs. 4(a) and 4(b) for 300 and 4.2 K, respectively. Without an external excitation voltage, the QTF is only driven by the thermal energy. The shape of the NSD has been explained by a driven, damped harmonic oscillator picture.[2,8] However, we find that although the data can be roughly de-

scribed by the Lorentzian line shape predicted by the harmonic oscillator model, a better fit can be obtained by using the equivalent circuit of the QTF described in Fig. 1, with the component values measured and fit by the impedance analyzer. The simulated noise spectra are shown in Fig. 4. At 4.2 K, the deviation from a simple harmonic oscillator is not as substantiated as that at 300 K.

We can use the thermal excitation to calibrate the sensitivity,[5] which is defined to be the ratio of the measured output signal (in volts) to the QTFs vibration amplitude (in meters). The sensitivity is a figure of merit, since it indicates whether the measured output signal is able to distinguish a small vibration. (A separate but related merit is the signal to noise ratio at the output.) The output signal, V_{rms}, to be fed into a lock-in amplifier, is obtained by integrating over the resonance frequency

$$V_{\mathrm{rms}}^2(\delta f) = \int_{f_0-\delta f/2}^{f_0+\delta f/2} df\ V_{\mathrm{total,rms}}^2. \tag{5}$$

The integration is centered at f_0 with a full width of δf. We find that $V_{\mathrm{rms}}(\delta f)$ saturates quickly as δf increases, reflecting the narrowness of the resonance. For example, at 4.2 K, V_{rms} reaches 90% of its saturated value (4.56×10^{-6} V) for $\delta f = 0.184$ Hz. The thermal vibration amplitude $\sqrt{\langle x^2\rangle}$ is estimated by equating[7] the thermal energy k_BT to the mechanical energy $k_Q\langle x^2\rangle$, where k_Q is the spring constant, k_B is the Boltzmann constant, and T is the absolute temperature. Given the dimensions and the Youngs modulus,[10] k_Q is calculated to be 2656 kg/s^2 and it is a weak function of temperature. We obtain a thermal mechanical vibration amplitude of 1.48×10^{-13} m. The sensitivity is therefore determined to be $V_{\mathrm{rms}}/\sqrt{\langle x^2\rangle} = 30.8\ \mu$V/pm. Similarly, at 300 K, due to thermal broadening, V_{rms} rises to 90% of its saturation value (3.5×10^{-6} V) with $\delta f = 1.25$ Hz. The calculated $\sqrt{\langle x^2\rangle}$ at 300 K is 1.25×10^{-12} m, yielding a sensitivity of 2.8 μV/pm. Cooling the QTF from 300 to 4.2 K increases the sensitivity by a factor of 11.

Our development of a cryogenic transimpedance amplifier facilitates the use of a quartz tuning fork in force sensing at cryogenic temperatures. In the future, we can further improve the performance. First, the frequency compensation[9] scheme, using an additional resistor and capacitor pair (R_c and C_c in Ref. 9) in the feedback loop to shift the zero and pole frequencies, can be applied to further extend the bandwidth to $\sim(1+A)/[R_f(C_{\mathrm{in}}+C_f)]$. Second, other wider gain-bandwidth second stage amplifiers could be used.

ACKNOWLEDGMENTS

This work at NRL is in part supported by the Office of Naval Research. The authors thank S. H. Moseley for discussion of amplifier implementation. C. H. Y. acknowledges support from ONR and LPS.

[1] G. Binnig, C. F. Quate, and Ch. Gerber, Phys. Rev. Lett. **56**, 930 (1986).
[2] T. R. Albrecht, P. Grütter, D. Horne, and D. Rugar, J. Appl. Phys. **69**, 668 (1991).
[3] K. Karrai and R. D. Grober, Appl. Phys. Lett. **66**, 1842 (1995).
[4] H. Edwards, L. Taylor, W. Duncan, and A. J. Melmed, J. Appl. Phys. **82**, 980 (1997).
[5] F. J. Giessibl, Appl. Phys. Lett. **73**, 3956 (1998).
[6] D. M. Eigler and E. K. Schweizer, Nature (London) **344**, 524 (1990).
[7] G. Giessibl, Appl. Phys. Lett. **76**, 1470 (2000).
[8] R. D. Grober *et al.*, Rev. Sci. Instrum. **71**, 2776 (2000).
[9] See, for example, C. L. Wyatt, D. J. Baker, and D. G. Frodsham, Infrared Phys. **14**, 165 (1974); W. J. Moore (unpublished).
[10] Raltron R38-32.768 kHz quartz tuning fork. The tuning fork is sealed hermetically in a can, and the vacuum seal survived multiple thermal cycling. The dimensions are: length = 3.636 mm, width = 540 μm, and thickness = 232 μm. The Young's modulus is 7.8×10^{10} N/m^2.
[11] Burr–Brown application note AB-050, "Compensate transimpedance amplifiers intuitively," available from http://www.ti.com.
[12] P. R. Gray and R. G. Meyer, *Analysis and Design of Analog Integrated Circuits* (Wiley, New York, 1977).